Proceedings of 12th IOE Graduate Conference
Peer Reviewed
ISSN: 2350-8914 (Online), 2350-8906 (Print)
Year: 2022 Month: October Volume: 12

Soil deformation behavior and SSI study by varying Poisson's ratio of granular soil

Santosh Katuwal [a], Archana Pandit [b], Anjali Shilpakar [c]

[a, b] *Kantipur City College, Purwanchal University, Nepal*
[c] *Department of Roads, Ministry of Physical Infrastructure and Transport, Government of Nepal*
[a] er.santoshkatuwal@gmail.com, [b] archanapandit@kcc.edu.np, [c] anjalishilpakar34@gmail.com

Abstract

The main aim of this study is to carry out the behavior of the soil and to perform soil-structure interaction investigation by varying the Poisson's ratio of the soil. For the study, dense type sand is taken due to its wide range variation of Poisson's ratio ranging from 0.2 to 0.4. The Poisson's ratio is increased by constant step of 0.05 (i.e. ν =0.20, 0.25, 0.30, 0.35, and 0.40) for the investigation. To study the soil deformation behavior, finite element analysis is performed using geotechnical investigation tool PLAXIS 3D Connect Edition V21. Based on the static load from the superstructure and its resulting soil deformation, spring stiffnesses are calculated at base of all columns. The computed springs from varying Poisson's ratio are modelled individually in structural analysis tool ETABS V20.0.0. Modal analysis using Ritz as well as Eigen vector method and non-linear modal time history analysis are carried out and results are studied thoroughly. It is found that deformation on soil is decreased while increasing Poisson's ratio of the soil; higher Poisson's ratio makes soil more rigid and resists both lateral as well as axial deformation of the soil. In addition, it is found from the analysis, the fundamental time period and damping of structure is increased as soil-structure integrated system is considered. The response spectrum from nonlinear time history analysis shows the change in Poisson's ratio has significatly low impact on dynamic response of the structure.

Keywords

Soil-Structure Interaction (SSI), FNA, Poisson's ratio, Interface element

1. Introduction

This study is carried out to investigate the deformation behavior of the soil subject to structural loading and to study soil structure interaction (SSI) effect by varying Poisson's ratio. In most of the cases, buildings get damaged due to settlement of the soil; therefore, responses on variation of Poisson's ratio are studied to investigate soil deformation behavior. The Poisson's ratio is varied linearly by the increment of 0.05 since Poisson's ratio captures the deformation ability of the soil along both lateral as well as in axial directions. Furthermore, soil structure interaction effect is studied by converting soil as equivalent spring model and dynamic analysis is performed and results are investigated thoroughly. Most of the structural analyses were carried out without considering the effect of soil that does not truly capture the structural response. Thus, this study is focused on SSI with variation of Poisson's ratio of the soil. In the study, soil deformation behavior and triaxial simulation test are analyzed using finite element analysis using PLAXIS 3D. The dynamic response of the structure is analyzed in ETABS using input strong ground motion recorded at Kirtipur during Gorkha earthquake,2015.

2. Soil Model

For the modeling of the soil, single layered homogeneous soil profile of dense sand is taken into consideration for the study. The linear elastic perfectly plastic Mohr-Coulomb soil profile is modeled based on soil parameters given by M. Budhu in the year 2020. The Mohr-Coulomb (MC) model is a widely used constitutive model that produces satisfactory numerical results for porous media, particularly frictional soils. The Mohr-Coulomb model is suitable for simple stress paths and predicts linear elastic-perfectly plastic behavior of the soil [1]. Coulomb's friction law is extended to universal states of stress by the MC yield condition. This condition, in fact, assures that Coulomb's friction law is followed in any plane within a material element. When expressed in terms of principle stresses, the whole MC yield condition consists of six yield functions (Equations 1 to 6) [2].

$$f_{1a} = \frac{1}{2}(\sigma_2^{'} - \sigma_3^{'}) + \frac{1}{2}(\sigma_2^{'} + \sigma_3^{'})sin\phi - Ccos\phi \leq 0 \quad (1)$$

$$f_{1b} = \frac{1}{2}(\sigma_3^{'} - \sigma_2^{'}) + \frac{1}{2}(\sigma_3^{'} + \sigma_2^{'})sin\phi - Ccos\phi \leq 0 \quad (2)$$

$$f_{2a} = \frac{1}{2}(\sigma_3^{'} - \sigma_1^{'}) + \frac{1}{2}(\sigma_3^{'} + \sigma_1^{'})sin\phi - Ccos\phi \leq 0 \quad (3)$$

$$f_{2b} = \frac{1}{2}(\sigma_1^{'} - \sigma_3^{'}) + \frac{1}{2}(\sigma_1^{'} + \sigma_3^{'})sin\phi - Ccos\phi \leq 0 \quad (4)$$

$$f_{3a} = \frac{1}{2}(\sigma_1^{'} - \sigma_2^{'}) + \frac{1}{2}(\sigma_1^{'} + \sigma_2^{'})sin\phi - Ccos\phi \leq 0 \quad (5)$$

$$f_{3b} = \frac{1}{2}(\sigma_2^{'} - \sigma_1^{'}) + \frac{1}{2}(\sigma_2^{'} + \sigma_1^{'})sin\phi - Ccos\phi \leq 0 \quad (6)$$

The yield function is the product of the friction angle and the cohesiveness of soil with respect to a given plastic. In main stress space, the individual yield function, $f_i = 0$ represents a fixed hexagonal cone as shown in figure 1. Figure 2 shows the Mohr-Coulomb failure criteria of the soil.

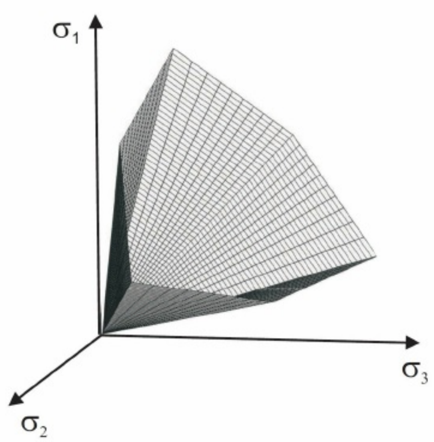

Figure 1: Mohr-Coulomb yield surface in principal stress [3]

The linearly elastic perfectly plastic Mohr Coulomb soil model consist of five input parameters, Young's modulus (E) and Poisson's ratio (ν) for soil elasticity; internal angle of friction (ϕ) and cohesion (c) for soil plasticity and angle of dilatancy (ψ). For modelling of soil, all parameters are kept constant except Poisson's ratio. Table 1 shows the various parameters required for soil modelling.

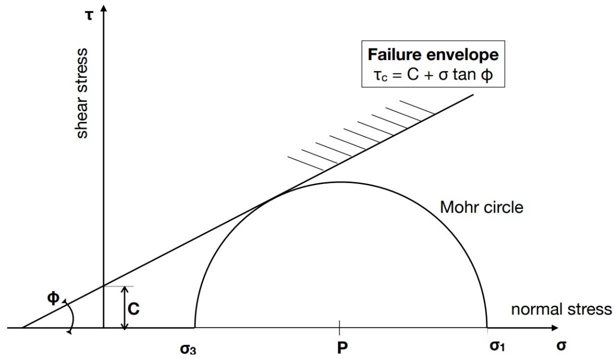

Figure 2: The MC failure criteria and Mohr's circle [4]

Table 1: Soil Model Parameters [5]

Sand Type	ν	(E)	(ϕ)	η	γ_{sat}	γ_d
Loose	0.15-0.25	10-20	29-34	60-80		
Medium	0.25-0.3	20-40	35-40	30-60	18-20	13-16
Dense	0.2-0.4	40-80	38-45	15-30		

Where, E is in MPa, ϕ is in degrees, porosity η is in %, γ_{sat} and γ_d are in kN/m^3. The void ratio (e) of soil is computed using porosity based on relation, $\eta = e/(1+e)$. In this study dense sand type soil is taken for the study. To investigate the behavior, all parameters except ν kept constant. Considered parameters for Mohr-Coulomb soil model are: E= 60 MPa, $\phi = 40^o$, $e = 0.25$, $\gamma_d = 15kN/m^3$, $\gamma_{sat} = 20kN/m^3$, and varying Poisson's ratio.

3. Dynamic Analysis

For the dynamic analysis of the structure using modal superposition method Ritz-vector analysis provides better result as compared Eigen vector analysis [6]. Both Ritz and Eigen vector analyses are performed to check the fundamental time period of the structure for all prepared soil-structure integrated model. Both

Eigen and Ritz vector analyses are performed simultaneously considering P-Delta effect for all models and fundamental period of vibration is compared. The FNA is performed using method developed by Ibrahimbegovic and Wilson [7] and Wilson [8]. The FNA captures nonlinear behaviors in predefined elements only; and the analysis performs based on modal superposition method. FNA is way efficient for structural systems having a limited number of nonlinearities, though is no limit on the number of nonlinear elements to be considered [9]. For a linear elastic structure with predefined nonlinear elements, the dynamic equilibrium equations can be written as:

$$M\ddot{u}(t)+C\dot{u}(t)+K_Lu(t)+R_{NL}(t)=R(t) \tag{7}$$

Where the terms M, K_L, C, and R_{NL}, are mass matrix, stiffness matrix of linear elastic element and Proportional damping matrix, and global resisting force vector for non-linear element respectively; $u(t)$, $\dot{u}(t)$, and $\ddot{u}(t)$ are relative displacement, velocity and acceleration with respect to time (t). Adding product of non-linear effective stiffness matrix K_N and $u(t)$ on both sides:

$$\begin{aligned} M\ddot{u}(t)+C\dot{u}(t)+K_Lu(t)+K_Nu(t) \\ =R(t)-R_{NL}(t)+K_Nu(t) \end{aligned}$$

$$M\ddot{u}(t)+C\dot{u}(t)+Ku(t)=\hat{R}(t) \tag{8}$$

Where, K=K_L+K_N and $\hat{R}(t)$=$R(t)-R_{NL}(t)+K_Nu(t)$

To perform FNA load dependent Ritz vector method is used to compute orthogonal mode shapes, ϕ. The equilibrium equation in modal form can be written as:

$$I\ddot{Y}(t)+\Lambda\dot{Y}(t)+\Omega^2Y(t)=F(t) \tag{9}$$

Where, I, Y, Λ and Ω are identity matrix, modal coordinate vector, modal damping matrix and modal frequency matrix respectively. The FNA method does not require complete set of all structural modes. Therefore, it is suggested to perform modal analysis using load dependent Ritz-vector method to determine a sufficient structural modes to represent structural response behavior [9].

Fast nonlinear analysis (FNA) is performed to analyze dynamic response of the structure using strong ground motion (Gorkha Earthquake) recorded at Kirtipur (see Figure 3).

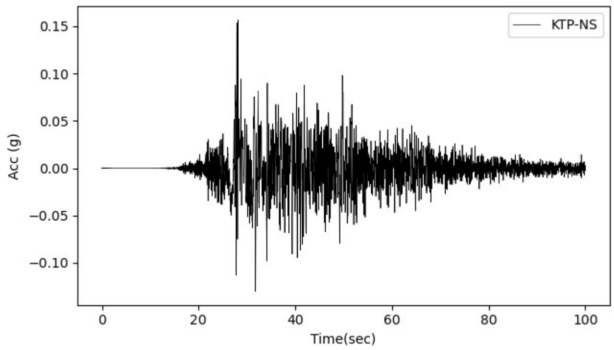

Figure 3: Strong motion seismogram recorded at Kirtipur during Gorkha earthquake

4. Modeling of structure and interface element

For the modelling of superstructure elastic type material having characteristic strength, unit weight, Poisson's ratio, Young's modulus of 25MPa, $25kN/m^3$, 0.2, $5000\sqrt{f_{ck}}(MPa)$ respectively are taken into consideration for the analysis of soil-structure integrated behavior. Furthermore, superstructure is modelled to study the dynamic characteristics of the structure. A square building of four bays on either directions and five stories are taken for the study. Figure 1 shows the soil structure integrated model prepared for the study. For the plastic analysis of soil-structure integrated model, beams and columns are modelled using beam element; slab and basement are modelled using plate element available in PLAXIS3D.

For the simulation of interaction between soil and structure, interface element is modelled to formulate slipping and gapping behavior between soil and structure. Two nodes of same coordinates are formulated to define interface element, the interaction between these nodes of common coordinate consist of two elastic-perfectly plastic springs. One spring is to model gap displacement and another is modelled to capture slip displacement [10].

5. Mesh generation

While computing using finite element method, the whole geometry divided into finite numbers of element using swept meshing method and calculation is carried out for all elements. Finite element method is numerical approach that divides complex geometry into finite numbers of simple elements, in which each

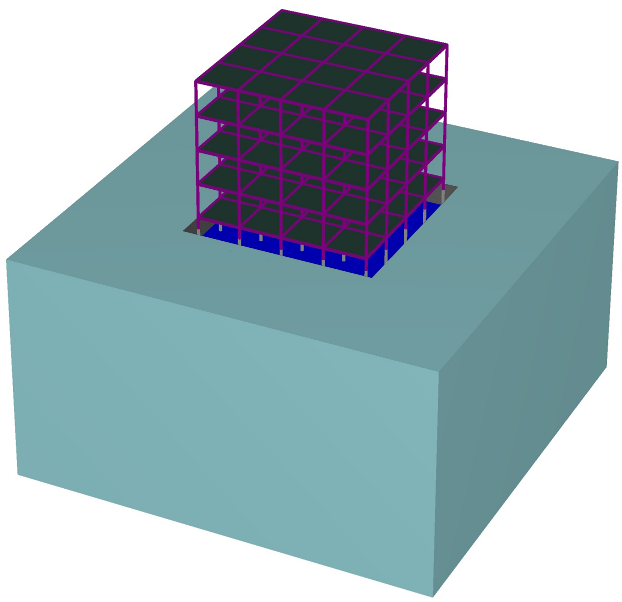

(a) Soil-structure integrated model

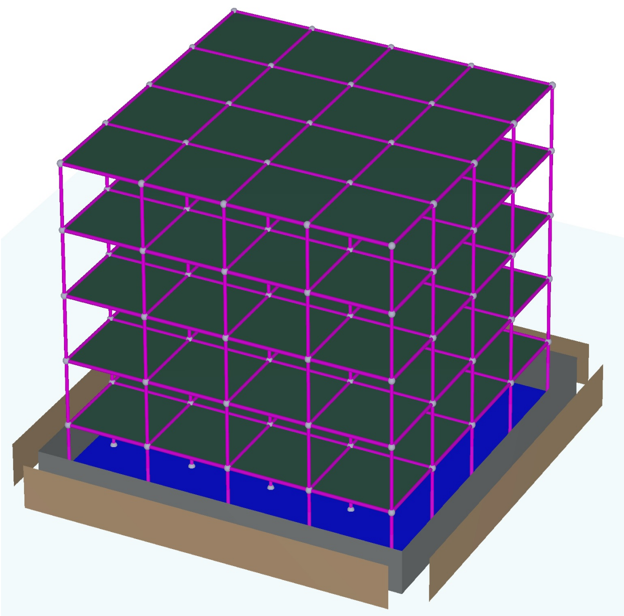

(b) Interface modelling

Figure 4: 3D finite element modeling

element consists of nodes and stress points. The computed results of each elements are assembled together to get the final response of the system. In this study 10 nodded tetrahedral element is used to mesh soil-structure integrated system, refer Figure 5.

6. Poisson's ratio

Poisson's ratio is elastic property that indicates deformation along lateral direction of force of

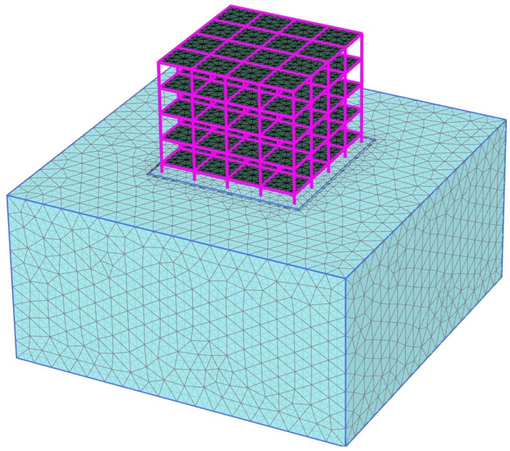

Figure 5: Generated mesh for finite element analysis

application [11]. Poisson's ratio is crucial for the analytical analysis and simulation for slope stability, earth pressure, soil settlement, shrinkage, swelling and bearing capacity. The relation between Young's modulus, bulk modulus (K) and Poisson's ratio E=3K(1-2ν) shows that maximum possible value of ν is 0.5 and if we see the expression E=2G(1+ν) [5, 11, 12], where G is shear modulus of the soil, minimum possible value of ν is -1. But negative value of Poisson's ratio is not applicable in the field of geotechnical engineering, negative Poisson's ratio is indication of lateral expansion due to application of axial tensile load and vice versa. Therefore, the value of ν lies within the range of 0 to 0.5, where 0 indicates it doesn't deform along lateral direction due to axial load and ν=0.5 represents change of deformation in lateral direction is half of deformation along axial direction.

In this study, effect of change in variation of Poisson's ratio of sandy soil is studied thoroughly. From the literature it is found that the value of ν of sandy soil varies from 0.2 to 0.4 [5]. Therefore, Mohr-Coulomb soil model is prepared by varying the value of ν from 0.2 to 0.4 in the increment of 0.05 by keeping other parameters (e.g., E, ϕ, c, ψ) constant to investigate the soil deformation pattern and structural response.

7. Spring element

Spring parameters are computed based on encountered force and resulting deformation at base of each columns using expressions: K_x=Q_{13}/u_x, $Ky = Q_{12}/u_y$ and $K_z = N/u_z$. Where, Kx, Ky and Kz are spring stiffness along X,Y and Z axes; u_x, u_y and u_z are deformation caused by shear forces Q_{13}, Q_{12}

and by axial force N respectively.

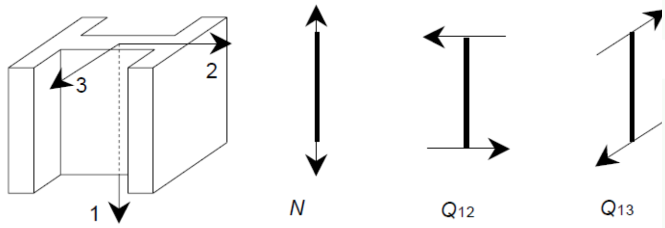

Figure 6: Shear and axial forces

Computed spring values from plastic analysis of soil-structure integrated model are modelled in ETABS for further dynamic study as shown in Figure 7.

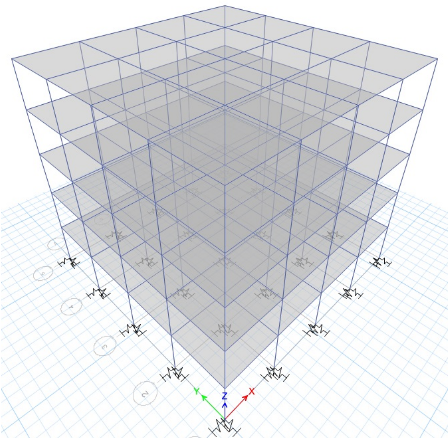

Figure 7: 3D structural modelling with spring support

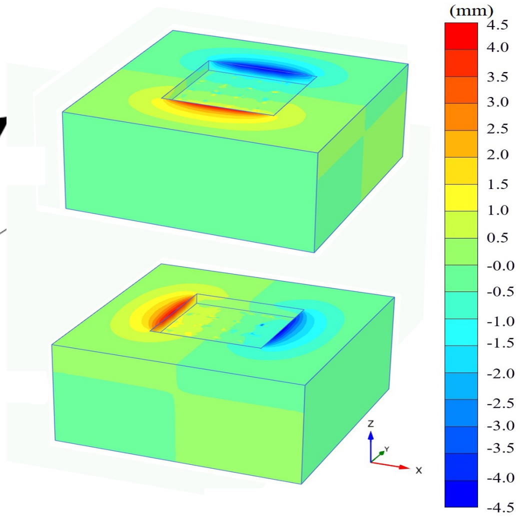

(a) Lateral soil deformation

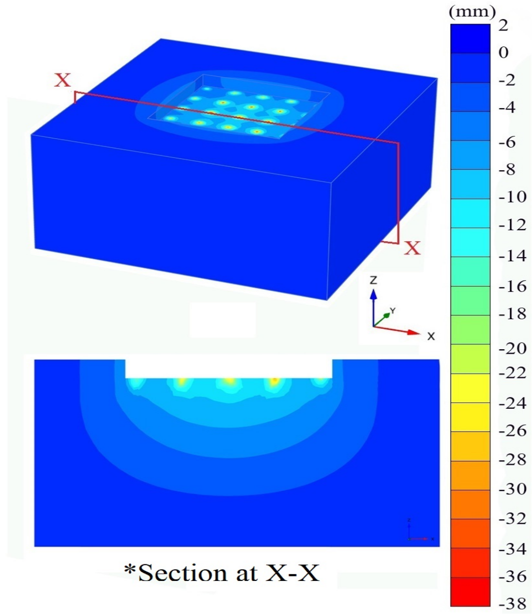

(b) Vertical soil deformation

Figure 8: Deformed soil mass ($\nu = 0.2$)

8. Results and Discussions

8.1 Soil deformation

In this study soil deformation pattern of a building having twenty-five columns are closely analyzed. Figure 9a and Figure 9b are the absolute lateral deformation of the soil along X and Y directions, Figure 9d is the deformation along vertical (Z direction) with varying Poisson's ratio from 0.2 to 0.4 in the incremental value of 0.05 for all twenty-five columns, and Figure 9c shows the average of absolute lateral deflection along X and Y directions. As we closely observe Figure 8 and 9, it can be found that the lateral deformation of soil decreases while increasing Poisson's ratio. Therefore, it can be stated that higher Poisson's ratio makes the soil more rigid and resists both lateral as well as axial deformations; though lateral deformation is very less as compared to axial deformation of the soil. Figures 8a and 8b show the deformed soil behavior in lateral and vertical directions respectively. Due to symmetric arrangement of the building, deformation along X and Y directions are similar.

8.2 Numerical analysis and result validation for soil deformation

To verify the soil deformation behavior, simulation of drained triaxial simulation test with compressive loading considering isotropic consolidation has been carried out for all soil models; the initial cell pressure for the soil is taken as 100kPa for the simulation.

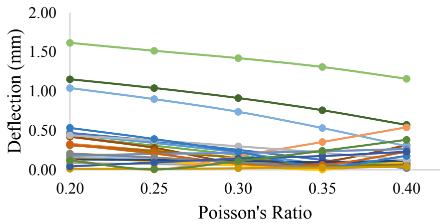

(a) X-direction

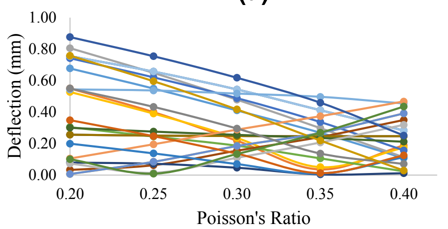

(b) Y-direction

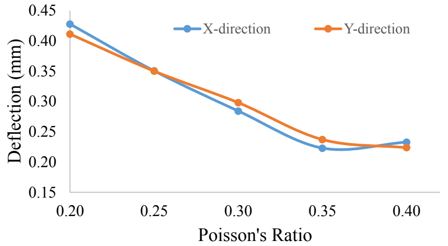

(c) Average of lateral direction

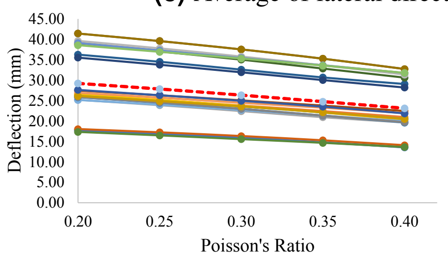

(d) Vertical direction

Figure 9: Absolute deformation of soil with varying Poisson's ratio

Figure 10 is the simulation model prepared for the analysis; Figure 11 is the Mohr-Coulomb circle with failure envelope of the prepared soil model for all range of Poisson's ratio.

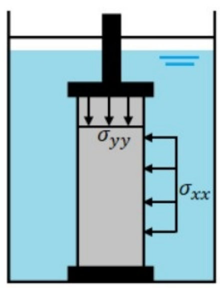

Figure 10: Triaxial test simulation model

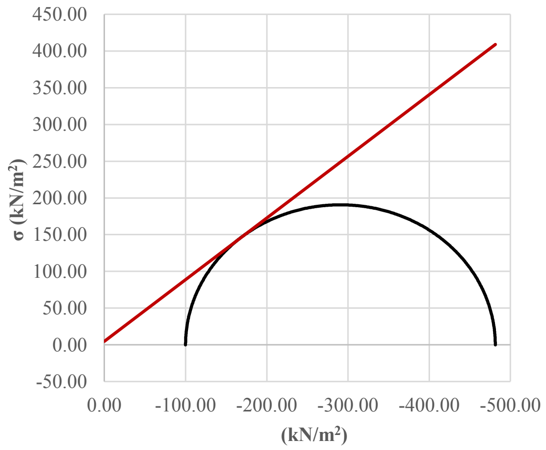

Figure 11: Mohr-Coulomb circle and failure envelope obtained from simulation

Figure 11 shows the Mohr-Coulomb circle is independent of Poisson's ratio of the soil. Therefore, to capture the deformation behavior of linear elastic perfectly plastic Mohr-Coulomb soil model, the relation between axial and volumetric strain are compared thoroughly from the triaxial test simulation. It is found that the volumetric strain significantly reduces as increase in Poisson's ratio. Therefore, it can be said that the increment of Poisson's ratio of soil makes soil rigid to deform.

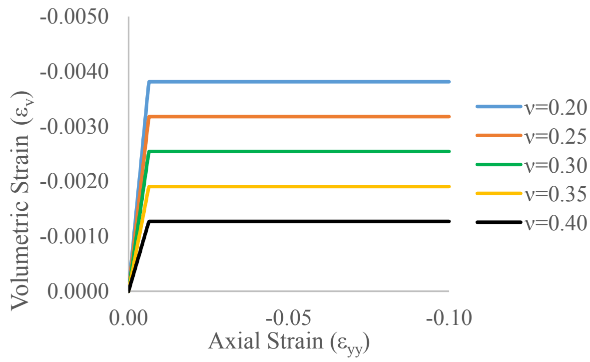

Figure 12: Relation between volumetric and axial strain obtained from triaxial test simulation for varying Poisson's ratio

8.3 Fundamental time period

The fundamental time period of vibration with P-Delta effect is studied using Eigen method and Ritz method for both fixed and varying spring support conditions. It is found that the fundamental time period of structure is increased as soil effect is considered rather than fixed-based support. Fundamental time period of structure is decreased as increase in Poisson's ratio due to decreased deformation ability of the soil. Ritz method of modal analysis is showing higher time period as compared to Eigen method of modal analysis for the particular structure. Comparison of fundamental time period of building is shown in Table 2.

Table 2: Fundamental time period comparison between by Ritz and Eigen vector analysis

Support condition	Fundamental Period (T1)	
	Ritz (sec)	Eigen (Sec)
Fixed	0.78	0.774
Spring (v=0.20)	1.605	1.569
Spring (v=0.25)	1.59	1.554
Spring (v=0.30)	1.588	1.552
Spring (v=0.35)	1.526	1.492
Spring (v=0.40)	1.527	1.492

8.4 Response of structure obtained from dynamic analysis

For the dynamic response evaluation of the structure, modal non-linear time history analysis (Fast Non-linear Analysis- FNA) is performed. Figure 13a to 13e are plots of response spectrum obtained from FNA on top floor of the structure. There is no significant variation is observed in the structural response while changing the Poisson's ratio of the soil. Structure with spring support representing soil has damped the vibration of the structure; Figure 13 shows that structure with fixed support condition has higher spectral acceleration as compared to spring support condition. Therefore, it can be said that the structure with soil-structure interaction effect increases damping as well as period of the vibration of the structural system.

9. Conclusion

It can be concluded from the analysis, increase in Poisson's ratio makes soil more rigid and resist deformation not only in axial direction but also towards lateral directions. In addition, it can be concluded from the soil structure interaction analysis, soil dampens the vibration of structure as well as increases the period of the vibration as compared to fixed-based structural system but variation in Poisson's ratio of the soil does not affect significantly in the dynamic behavior of the structure.

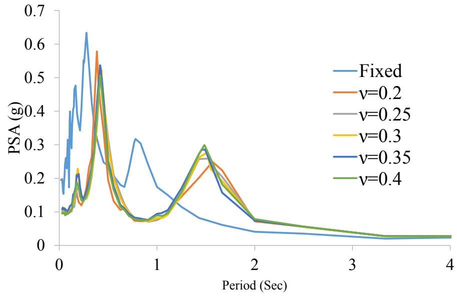

(a) First floor

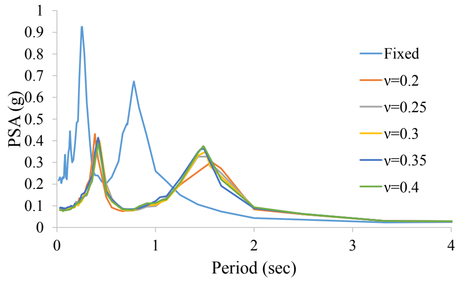

(b) Second floor

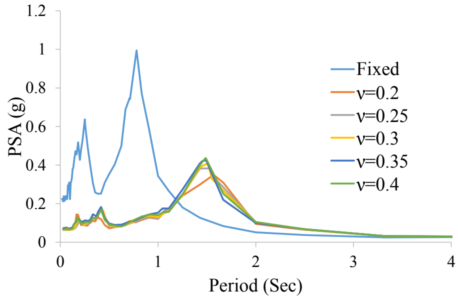

(c) Third floor

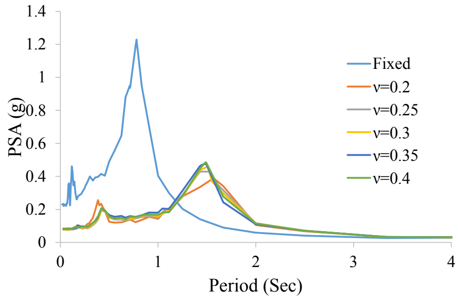

(d) Fourth floor

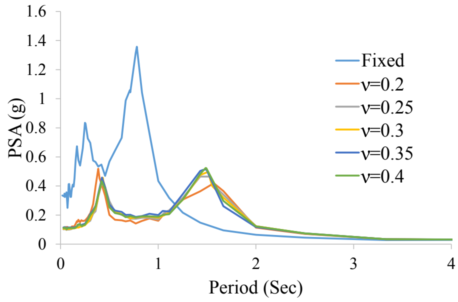

(e) Fifth floor

Figure 13: Response spectrum plot at different floor level

Acknowledgments

The authors would like to express heartfelt gratitude to everyone associated with this research. The authors are also thankful to the faculty of the Civil Engineering, Kantipur City College for their support in making this research a success, both directly and indirectly.

References

[1] KN Vakili, T Barciaga, AA Lavasan, and T Schanz. A practical approach to constitutive models for the analysis of geotechnical problems. In *The Third International Symposium On Computational Geomechanics (ComGeo III), at Krakow, Poland*, volume 1, pages 738–749, 2013.

[2] Ian Moffat Smith, Denwood Vaughan Griffiths, and Lee Margetts. *Programming the finite element method*. John Wiley & Sons, 2013.

[3] RBJ Brinkgreve, WM Swolfs, and E Engin. Plaxis 2d 2010 material models manual. *PLAXIS BV*, 2011.

[4] Daniel Hestroffer, Paul Sánchez, Lydie Staron, A Campo Bagatin, Siegfried Eggl, Wolfgang Losert, Naomi Murdoch, Eric Opsomer, Fahrang Radjai, Derek C Richardson, et al. Small solar system bodies as granular media. *The Astronomy and Astrophysics Review*, 27(1):1–64, 2019.

[5] Muni Budhu. *Soil mechanics and foundations*. Number 1. Wiley,, 2020.

[6] BASICAYS REF and ER ENCE MANUAL. Sap2000®. 1978.

[7] Adnan Ibrahimbegovic and Edward L Wilson. Simple numerical algorithms for the mode superposition analysis of linear structural systems with non-proportional damping. *Computers & structures*, 33(2):523–531, 1989.

[8] LW Edward. Static and dynamic analysis of structures: A physical approach with emphasis on earthquake. [m]. *USA: Computers and structures Inc*, 2004.

[9] Y Lu and GR Morris. Assessment of three viscous damping methods for nonlinear history analysis: Rayleigh with initial stiffness, rayleigh with tangent stiffness, and modal. In *Proceedings, Sixteenth World Conference on Earthquake Engineering*, number 1170, 2017.

[10] RBJ Brinkgreve, E Engin, WM Swolfs, D Waterman, A Chesaru, PG Bonnier, and V Galavi. Plaxis 3d 2012. *Plaxis bv*, 2012.

[11] Sannith Kumar Thota, Toan Duc Cao, and Farshid Vahedifard. Poisson's ratio characteristic curve of unsaturated soils. *Journal of Geotechnical and Geoenvironmental Engineering*, 147(1):04020149, 2021.

[12] Frederic Gladstone Bell. *Engineering properties of soils and rocks*. Elsevier, 2013.